Journal of Biomechanics 191 (2025) 112915

Contents lists available at ScienceDirect

Journal of Biomechanics

journal homepage: www.elsevier.com/locate/jbiomech

Medial gastrocnemius muscle and aponeurosis shear wave velocity and morphological changes after Achilles tendon rupture: A 1-year follow-up study

Ra'ad M. Khair [a,*], Maria Sukanen [a], Neil J. Cronin [a,b], Taija Finni [a]

[a] Faculty of Sport and Health Sciences, Neuromuscular Research Center, University of Jyväskylä, Jyväskylä, Finland
[b] School of Education & Science, University of Gloucestershire, Gloucestershire, UK

ARTICLE INFO

Keywords:
Elasticity
Injury
Triceps surae
Aponeurosis
Rupture
Shear wave elastography

ABSTRACT

Achilles tendon rupture (ATR) alters stiffness of the tendon and other structures within the triceps surae muscle–tendon unit. Although stiffness of the tendon has been studied after rupture, regional adaptations of the medial gastrocnemius (MG) muscle and aponeurosis mechanical properties are unknown. Therefore, we assessed changes in MG muscle and aponeurosis shear wave (SW) velocity and morphology during a 1-year follow-up after unilateral ATR. Twenty-three (17 males, 6 females) participants were assessed for SW velocity of MG muscle and aponeurosis and morphological properties at 2, 6 and 12 months at rest. Linear mixed models were used to investigate the differences between limbs at different time points, and partial correlations controlled for age to explore associations between SW velocity and morphological properties. Regional SW stiffness of the injured MG muscle and aponeurosis were lower at 2 months but recovered by 6 months after ATR. When comparing limbs, MG muscle and aponeurosis SW velocity were lower in the injured limb at 2 months with a mean difference of −0.34 m/s (−0.48 to −0.21 m/s, t = -5.10), and −1.6 m/s (−2.39 to 0.89 m/s, t = 4.38). SW velocity did not differ at the muscle or aponeurosis between limbs at 6 or 12 months. Fascicle length of the MG muscle was negatively correlated with SW velocity of the MG muscle ($r = -0.25$, $p = 0.041$) and positively correlated with aponeurosis SW velocity ($r = 0.29$, $p = 0.018$). The remodelling of the MG muscle to shorter fascicles might help to enhance stiffness and maintain tension at the muscle.

1. Introduction

Force exerted by a muscle is transmitted readily through the surrounding collagen-rich connective tissues (Huijing, 2003), including aponeurosis and free tendon, to reach the bone and facilitate locomotion. Although some force may be transmitted in cross-fiber directions (Finni et al., 2017; Huijing, 2003), the main pathway of force is the stiffest myotendinous structure. Stiffness (i.e. ratio of length to force change) is an important factor for muscle energetics as it affects rate of force development, force production and efficiency of locomotion (Bojsen-Møller et al., 2005; Ettema and Huijing, 1994; Monte and Zignoli, 2021; Roberts, 2016). The stiffness of tendinous tissue can be altered by acute injuries such as tendon rupture (Agres et al., 2015; McNair et al., 2013) and can influence the structure and function of the muscle in series; for example, fascicle length is inter-related with tendon compliance and gait efficiency (Bohm et al., 2021; Lichtwark and Wilson, 2008; Monte et al., 2020).

Passive mechanical properties of the muscle in series have important functional relevance, affecting a muscle–tendon unit's (MTU) capacity to execute movements across large ranges of motion with minimal metabolic energy expenditure (Blazevich, 2019). In endurance runners, higher plantar flexor passive stiffness was found to be associated with better running economy (Ueno et al., 2017). Moreover, passive stiffness of the plantar flexors may be a reflection of muscle parallel elastic component characteristics rather than tendinous tissue (Kubo et al., 2001).

Shear wave elastography (SWE) is a non-invasive technique that allows regional assessment of soft tissue mechanical properties (Bercoff et al., 2004; Bernabei et al., 2020; Eby et al., 2013). SWE provides a surrogate measure of tissue stiffness by tracking shear waves (SW) generated by radiation pulses (Bernabei et al., 2020). Tissue stiffness is determined based on the propagation velocity (m/s) of the SWs. Recent

* Corresponding author at: Faculty of Sport and Health Sciences, University of Jyväskylä, PO BOX 35 (LL177), 40014 Jyväskylä, Finland.
E-mail addresses: raad.m.khair@jyu.fi (R.M. Khair), maria.e.sukanen@jyu.fi (M. Sukanen), neil.j.cronin@jyu.fi (N.J. Cronin), taija.m.juutinen@jyu.fi (T. Finni).

https://doi.org/10.1016/j.jbiomech.2025.112915
Accepted 14 August 2025
Available online 15 August 2025

studies suggest a relationship between plantar flexor muscle stiffness measured at rest with SWE and during passive lengthening (Chino and Takahashi, 2016). Additionally, lower SW velocity of the medial gastrocnemius (MG) muscle were documented following a 12-week muscle mediated stretching program (Andrade et al., 2020), and after acute static stretching (Akagi and Takahashi, 2013), in agreement with expected muscle stiffness adaptation to stretching. These studies indicate that SW technology is sensitive enough to detect adaptations resulting from exercise or injuries such as Achilles tendon rupture (ATR) (Aubry et al., 2011). However, careful interpretation is advised as SW stiffness measurements rely on the assumptions that tendons are linearly elastic, homogenous and isotropic which might not be fully met *in vivo* (Bercoff et al., 2004; Khair et al., 2024).

Studies evaluating SW velocity of the Achilles tendon (AT) after rupture have found lower SW velocity in the injured limb that increases to comparable levels of the un-injured side within 12-weeks (Yoshida et al., 2023). Our recent study showed association between SW velocity and toe region of the tendon force–elongation curves one year after ATR (Khair et al. 2024). Furthermore, the stiffness based on force–elongation curves was different between the shorter free AT compared to the longer MG tendon (Khair et al., 2024). Thus, there may be regional differences in tissue stiffness that are inherent but also influenced by the recovery state.

It is well established that ATR changes the contractile component of the triceps surae MTU. In the first weeks following rupture, the length of the AT increases, which prompts remodelling of the MG muscle, characterized by a reduction in fascicle length (Baxter et al., 2018; Hullfish et al., 2019). These adaptations in the structure of the MG muscle are critical to enable the ruptured limb to operate within a near-optimal operating range, albeit with a narrower range of active force generation (Stäudle et al., 2020). In the context of the muscle force–velocity relationship, assuming a similar contraction velocity shorter fascicles are expected to produce less force than longer fascicles (Hill, 1953). Those changes in function and structure of the MG and the triceps surae MTU can alter the stiffness of the muscle, aponeurosis and tendon, yet such changes after ATR are poorly understood.

Therefore, the objective of this study was to examine changes in MG muscle and aponeurosis SW velocity and MG muscle morphology during a 1-year follow-up after unilateral ATR. We hypothesized that SW velocity of the MG muscle and aponeurosis would be lower on the injured side than on the contralateral side at 2 months, then increase to be similar at 6 months, and exceed that of the un-injured side at 12 months after rupture (Yoshida et al., 2023). Additionally, to understand the interplay between contractile and tendinous tissue, we explored the associations between SW velocity, morphological properties of the MG muscle and plantar flexion maximum voluntary torque (MVC).

2. Methods

In total, 23 participants (6 females; 41 ± 10.6 years, 178 ± 9.6 cm, 87 ± 17.4 kg) with unilateral ATR were recruited within a clinical cohort study (NoARK, trial registration: NCT03704532). Participants were diagnosed within 14 days of the rupture using guidelines by the American Academy of Orthopaedic Surgeons and received non-surgical treatment. Inclusion criteria were a minimum of 2 of the following 4 criteria: a positive Thompson test, decreased plantarflexion strength, presence of a palpable gap, and increased passive ankle dorsiflexion with gentle manipulation (Surgeons, 2009). Participants who suffered avulsion fracture or a re-rupture were excluded from the analysis. Participants were treated non-surgically with early mobilisation (Reito et al. 2018). This study was approved by the Ethics committee of Central Finland health care district (2U/2018). Participants signed an informed consent explaining the details of the study, possible risks, and gave permission to use data for research purposes. Participants were tested (mean ± SD) 2.2 ± 0.4, 6.1 ± 0.3, and 12.3 ± 05 months after rupture.

2.1. Laboratory test protocol

B-mode ultrasound images were acquired using a 6-cm linear probe (UST-5712; 7.5 MHz, Aloka, Tokyo, Japan) while participants laid in prone position with a relaxed ankle joint angle, and feet over the end of a table. Ultrasonography was used to locate the most distal point of the MG muscle–tendon junction and the proximal edge of the calcaneus, both of which were marked on the skin. Then, the distance was measured with a measuring tape following the curvature of the AT (Barfod et al., 2015). Images to calculate fascicle length and cross-sectional area (CSA) were captured halfway between the muscle–tendon junction and the crease of the knee, at the point where the deep and superficial aponeuroses of the muscle run parallel (Bolsterlee et al., 2016). CSA images were taken using the extended field of view function from the same muscle location with the knee flexed to 90 ° (Khair et al., 2022). Two images were taken, and average values were used for further analysis.

Supersonic shear wave elastography (Aixplorer Supersonic Imagine, v. 12.3.1 Aix-en-Provence, France) was used to record shear wave velocity (m/s) of the MG muscle and aponeurosis (Bercoff et al. 2004) with a linear 38 mm probe (2–10 MHz, SL10-2). Measurements were performed with a custom musculoskeletal pre-setting (penetration mode, smoothing level 5, persistence off, opacity 100 %) with the participant in prone position and ankles relaxed over the end of the table (Fig. 1). Taking into account the sensitivity of SWE to passive tension, participants relaxed in a prone position for 3 min prior to imaging to unload tension on the triceps surae MTU. Once relaxed, it is reasonable to assume that this position represents the passive state of the plantar flexors. Additionally, this approach is commonly used in studies assessing SWE properties of the triceps surae (Chino and Takahashi, 2016; Coombes et al., 2018; DeWall et al., 2014).

For MG muscle, the probe alignment was determined at 50 % of muscle belly length, where multiple fascicles and both superficial and deep aponeurosis were visible in sagittal view. For the aponeurosis, images were acquired from the most distal point of MG muscle. The probe was positioned perpendicular to the skin with a clear view of both aponeurosis and proximal MG subtendon. The deep aponeurosis was assessed as it represents the proximal extension of the AT (Shin et al., 2009). The elasticity range was adjusted according to the individual MG and aponeurosis properties to visualize changes in the SWE colourmap while avoiding saturation (maximum device range 0–16.3 $m \times s^{-1}$). Videos ranged between 3–5 s per condition. Intra-rater reliability of SW imaging was tested for one rater with an additional pilot sample ($n = 8$) with a minimum of 24 h between two trials. Reliability of SW imaging for MG aponeurosis was ICC 0.87 (95 % CI 0.41–0.98), CV of 5.9 %, SEM 0.33 m/s and MDC 0.9 m/s, and for the MG muscle belly ICC 0.77 (95 % CI 0.14–0.96), CV of 3.7 %, SEM 0.09 m/s and MDC 0.2 m/s.

After the ultrasound measurements, participants sat in a custom-made ankle dynamometer (University of Jyväskylä, Finland) with the hip at 120°, knee at 0°, and the ankle and first metatarsophalangeal joints fixed at 90° and 0° respectively. First, participants performed a series of submaximal isometric contractions as warm-up and familiarization. Then, participants were instructed to perform MVC's, with verbal encouragement provided to ensure maximal effort. Participants performed at least 3 ramp isometric contractions and the trial with the highest peak torque was used. Data were sampled at 1KHz via a 16-bit A/D board (Power 1401, Cambridge Electronic Design, Cambridge, UK) connected to the lab computer, and signals were recorded using Spike2 software (Cambridge Electronic Design, Cambridge, UK).

2.2. Data analysis

B-mode image analysis was performed using ImageJ (1.44b, National Institutes of Health). Reliability of these measurements was established previously (Khair et al., 2022).

SW videos were processed using semi-automated software developed

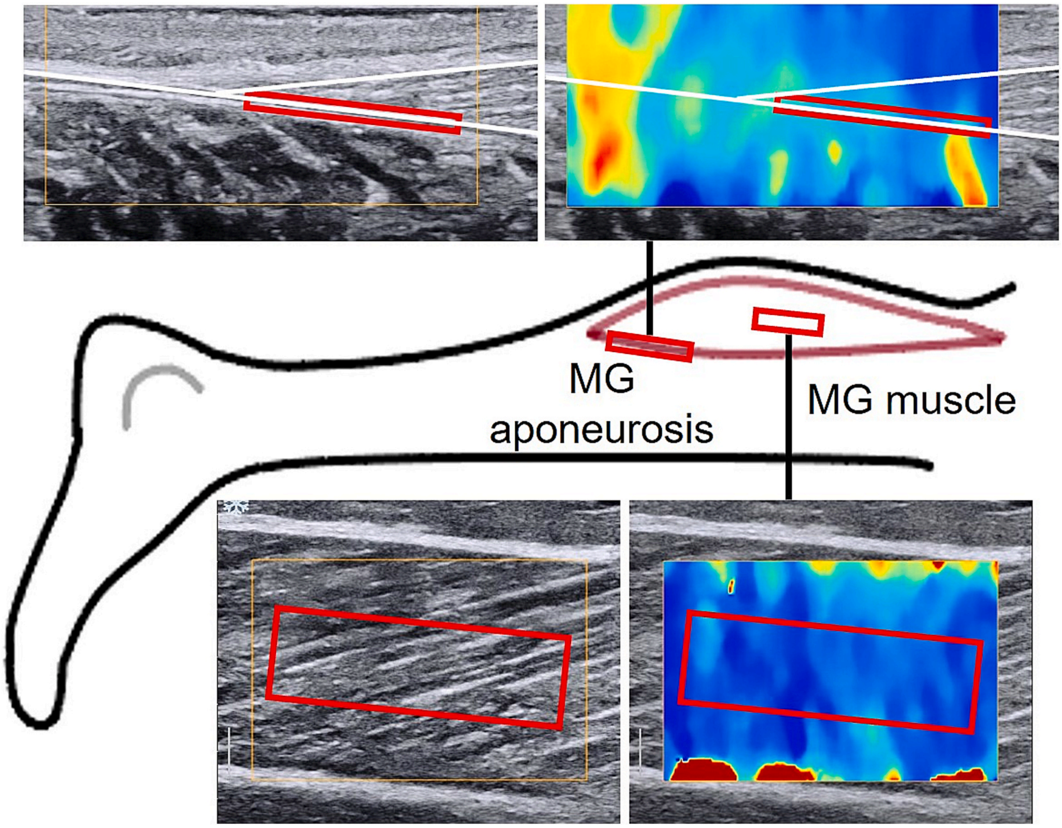

Fig. 1. Schematic representation of the SW measurement protocol. SW velocity was assessed at the MG muscle belly (below), and aponeurosis (above) from prone position with foot relaxed over the end of the table.

in MATLAB (ElastoGUI, University of Nantes, France). Accepted thresholds for saturation and void levels were < 1 % and < 0.1 %, respectively. The area of the MG aponeurosis was chosen to cover the distal deep aponeurosis of the MG (Fig. 1). MG muscle belly area was chosen to cover the largest area possible while avoiding artifacts. For further details about this analysis, readers are referred to the supplementary material appendix 1.

2.3. Statistical analysis

Linear mixed models were used to investigate the effects of time (2, 6, and 12 months) and limb condition (injured and un-injured) on the MG tendon and fascicle length, CSA, and SW velocity of MG muscle and aponeurosis. Models were built in JASP (JASP 0.18, Netherlands) with time and limb condition as fixed effects variables and participant as random factor. Restricted maximum likelihood with Satterthwaite approximation was used since it produces acceptable type 1 error for small sample sizes (Luke, 2017). Linear mixed models were used as it allows for the inclusion of all available data without the need for imputation or case-wise deletion, assuming data are missing at random. Missing at random assumption was evaluated by modelling the probability of missingness using logistic regression based on observed variables. Our main interest was in the interactions between time and limb condition on the structural and mechanical properties of the MG muscle. Analysis was followed by pairwise Bonferroni-adjusted comparisons. Skewness and kurtosis were checked to insure the normality of the data. The level of significance was set at $p < 0.05$, and descriptive data are reported as mean (SD). Data from 6 and 12 months were used to perform partial correlations controlled for age to explore the relationship between SW velocity, MVC and morphological properties. The analysis was performed for the injured and the un-injured limbs separately, and finally for both limbs pooled together.

3. Results

Six participants did not attend their biomechanical assessment at the 2-month follow-up, seven at 6 months, and five at 12 months. As a result, the final dataset included 102 data points: 34 at 2 months, 32 at 6 months, and 36 at 12 months. Logistic regression analysis supported the assumption that the data were missing at random.

Table 1 shows the mean values at three timepoints. At two months, MG tendon length was longer but fascicle length, muscle CSA, muscle SWV and aponeurosis SWV were lower in the injured compared to the un-injured limb. These limb-related differences persisted throughout the year in MG tendon length, MG fascicle length and MG CSA.

MVC of the injured limb was lower at 6 months (mean difference (95

Table 1
Descriptive data of the measured variables.

	2 months		6 months		12 months	
	Un-injured	*Injured*	*Un-injured*	*Injured*	*Un-injured*	*Injured*
MG tendon length (cm)	17.7 ± 1.7	19.4 ± 2.0[a]	18.2 ± 1.9	20.1 ± 1.8[a]	17.8 ± 1.9	19.9 ± 1.8[a]
Fascicle length (cm)	4.9 ± 0.7	4.4 ± 0.5[a]	5.0 ± 0.7	4.3 ± 1.1[a]	5.2 ± 0.9	4.1 ± 0.9[a]
CSA (cm^2)	15.4 ± 4.5	12.7 ± 3.4[a]	15.9 ± 5.4	13.4 ± 4.2[a]	16.3 ± 5.6	13.8 ± 4.7[a]
MG aponeurosis SW velocity (m/s)	6.4 ± 1.3	4.8 ± 0.9[a]	6.9 ± 1.4	6.7 ± 1.8[b]	6.9 ± 1.5	6.8 ± 1.7[b]
MG muscle SW velocity (m/s)	2.1 ± 0.2	1.7 ± 0.3[a]	2.1 ± 0.3	1.9 ± 0.3	2.0 ± 0.3	2.0 ± 1.6[b]

[a] denotes statistical differences between the injured and un-injured limbs, while [b] denotes temporal changes within limbs the 2 months times point to 6 and 12 months.

%CI) of −78.3 Nm, [-102.2 to −54.46 Nm], t = -6.80), and 12 months (−66.8 Nm, [-90.7 to −42.97 Nm], t = -5.81) compared to the un-injured limb. MVC increased in both limbs from 6 months to 12 months, with a mean difference (28.2 Nm, [11.98 to 44.37 Nm], t = 3.57) in the un-injured, and (39.7 Nm, [23.49 to 55.86 Nm], t = 5.04) in the injured limb.

In the linear mixed model for MG aponeurosis SW velocity, a significant interaction was observed between limb condition and time ($p = 0.002$). Compared to the un-injured limb, the injured limb aponeurosis SW velocity was lower at 2 months (−1.6 m/s, [-2.39 to 0.89 m/s], t = 4.38) and increased to comparable levels 6 months after rupture (Fig. 2). Within the injured limb, MG aponeurosis SWV increased 1.7 m/s from 2 to 6 months (−2.49 to −0.93 m/s, t = -4.43) and reached 6.8 ± 1.7 m/s at 12 months (Fig. 2).

The linear mixed model for MG muscle SW velocity showed a significant interaction between limb condition and time ($p < 0.001$). In the injured limb, MG muscle SW velocity was lower at the 2 months time-point compared to the un-injured (−0.34 m/s [-0.48 to −0.21 m/s], t = -5.10) and compared to the injured limb at 12 months (−0.31 m/s [-0.47 to −0.15 m/s], t = -3.93) (Fig. 2).

3.1. Associations between SW velocity, MVC and MG morphological properties

Data from 6- and 12 months were combined for this analysis since no within limb differences were detected between these two time points. In the un-injured limb, SW velocity of the MG muscle negatively correlated with MG fascicle length (r = -0.51 [-0.74 to −0.18]). MVC peak torque correlated with fascicle length (r = 0.55 [0.27 to 0.76]) and CSA (r = 0.65 [0.42 to 0.79]) of the MG muscle (Figs. 3 and 4).

In the injured limb, SW velocity of the aponeurosis correlated with MG fascicle length (r = 0.35 [0.02 to 0.67]). MVC in the injured limb correlated with fascicle length (r = 0.52 [0.35 to 0.69]) and CSA (r = 0.48 [0.25 to 0.69]) of the MG muscle.

When both limbs were pooled together, fascicle length of the MG muscle was negatively correlated with SW velocity of the MG muscle (r = -0.25 [-0.48 to 0.010]) and positively correlated with aponeurosis SW velocity (r = 0.29 [0.07 to 0.5]). MVC showed positive correlations with SW velocity of the aponeurosis (r = 0.29 [0.10 to 0.26]), fascicle length (r = 0.66 [0.53 to 0.76]) and CSA (r = 0.56 [0.39 to 0.70]) of the MG muscle.

4. Discussion

The present study assessed changes in SW velocity at the MG muscle and aponeurosis to understand the interplay and adaptations of contractile and tendinous tissue during a 1-year follow-up in patients with unilateral ATR. As expected, SW velocity in both the MG muscle belly and aponeurosis of the injured limb was lower compared to the un-injured limb at 2 months, possibly due to the lack of tensile stimulus in the early immobilization period. By 6 months, SW velocities had increased to levels comparable to the un-injured limb. An additional novel finding of this study was that longer MG fascicle length was associated with lower SW velocity of the MG muscle and higher SW velocity at the aponeurosis.

Our findings show that the MG muscle of the injured limb had a lower SW velocity at 2 months compared to the un-injured side. Given that muscles are sensitive to mechanical tension (de Boer et al., 2008), it is plausible to assume that the lower SW velocity of the muscle is due to loss of tensile tension caused by immobilization and increased length of the tendon after rupture. Six months after rupture, there was no difference between limbs in MG muscle SW velocity. This could be a consequence of tensile loading with progressive rehabilitation, prompting an increase in muscle SW velocity in addition to the re-modelling of the MG muscle to shorter fascicles (Hoeffner et al., 2023; Khair et al., 2022). We observed an inverse relationship between fascicle length and SW velocity of the MG muscle. Hence, the data suggest that higher SW velocity after 2 months may be partly attributed to shorter MG fascicle length. Because of the increased length of the tendon after rupture, shorter fascicles may be necessary to maintain tension at a level comparable to the un-injured limb (Hoeffner et al., 2023).

The finding that SW velocity of the aponeurosis was lower at 2 months and increased to similar levels to that of the un-injured limb at 6 months (Fig. 2) is consistent with previous studies that assessed AT mechanical properties after rupture. In the first 8 weeks after rupture, SW velocity at the free tendon was found to be lower compared to the contralateral limb (Chen et al., 2013; Sukanen et al., 2024). By 12 weeks, SW velocity has been reported to be comparable with SW values of the un-injured limb (Yoshida et al., 2023). Thus, it may be hypothesized that the aponeurosis follows a similar recovery pattern as the free tendon. However, it should be noted that the aponeurosis has contraction-dependent and different mechanical properties compared to tendon (Lieber et al., 1991), with studies showing a more compliant behaviour in the aponeurosis than that of the tendon (Finni et al., 2022;

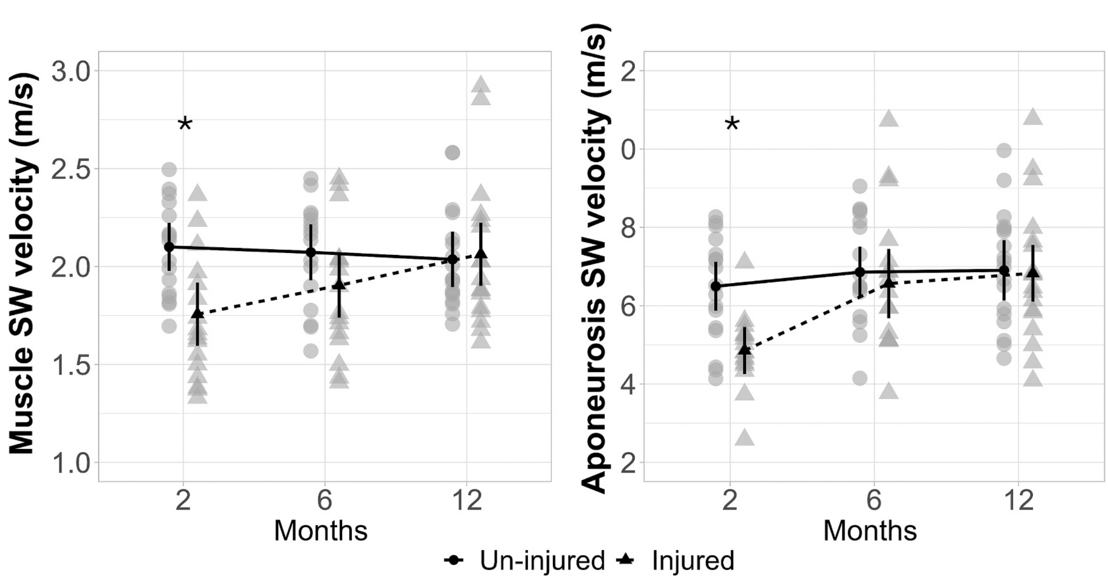

Fig. 2. Line plots showing means ± SD of SW velocities measured at the MG muscle belly (left) and MG aponeurosis (right). Dashed lines and triangles indicate the injured limb, while solid lines and circles represent the un-injured limb. *Significant difference between limbs ($p < 0.05$).

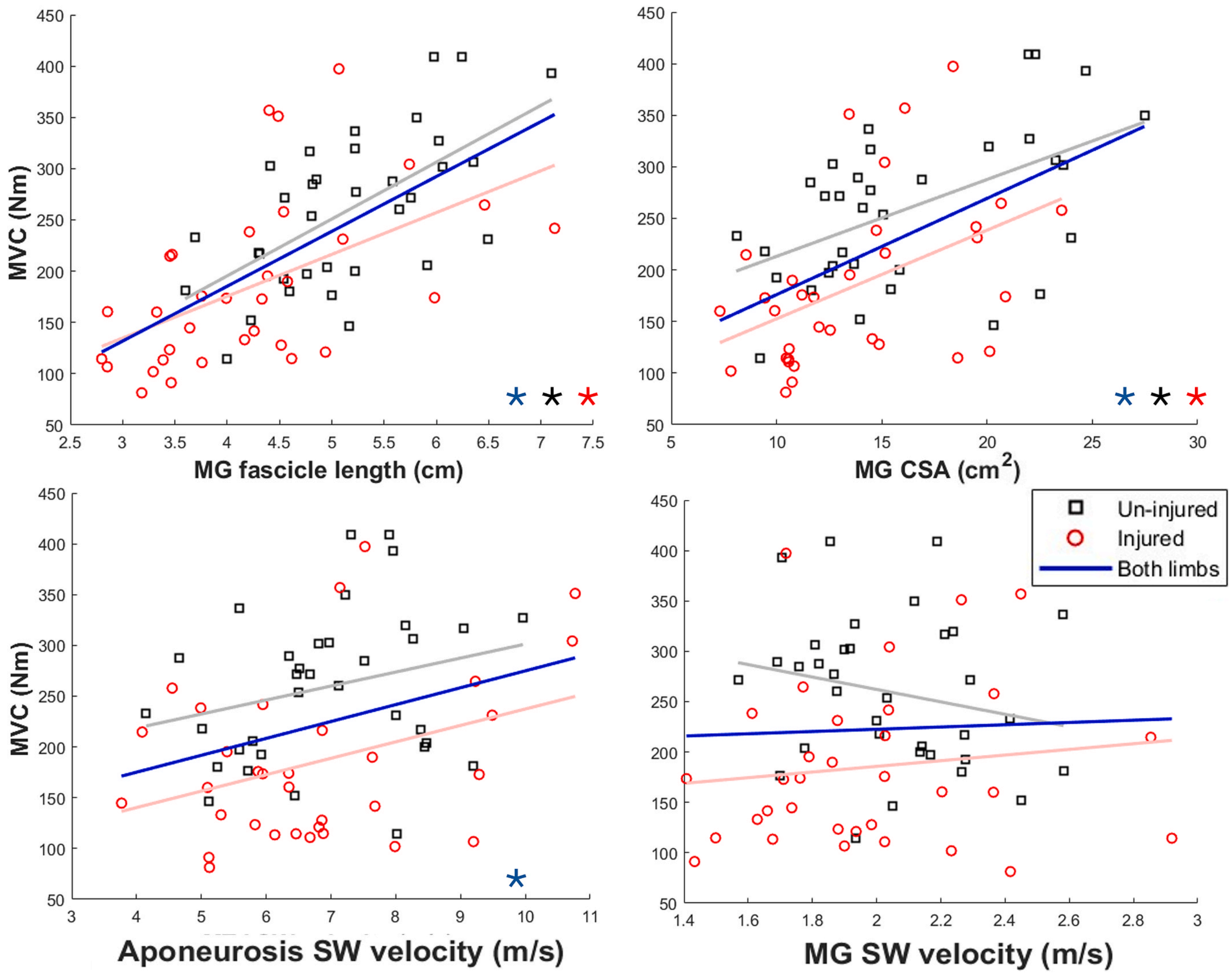

Fig. 3. Scatterplots and regression lines of the correlations between plantar flexion maximum voluntary torque (MVC) and measured variables at 6 and 12 months. * Significant correlation $p < 0.05$, *colour coded as follows: black for un-injured limb, red for injured limb, and blue for both limbs combined. (For interpretation of the references to colour in this figure legend, the reader is referred to the web version of this article.)

Finni and Komi, 2002; Ross et al., 2024). Additionally, the alignment of the AT and aponeurosis is complex and not strictly in series (Epstein et al., 2006) but these concepts fall outside the scope of this study. In the long-term, increased stiffness in the tendon and aponeurosis may help to reduce force production impairments resulting from ATR (Städule et al., 2020). Indeed, we found a positive correlation between the aponeurosis SW velocity and absolute plantar flexion torque. It is beneficial for the MTU if the tendinous tissue remodels to a higher stiffness, as this facilitates active force generation in a smaller operating range.

In the injured limb, MG CSA was smaller with shorter fascicles 1-year after rupture. These structural changes in the MG have clear functional implications, particularly affecting the maximum plantar flexion torque (Fig. 3). Consistent with our previous findings (Khair et al., 2022), the remodelling of the MG muscle accompanied lower force production capacity in the injured limb. Notably, in the injured limb, MG had a slight increase in CSA accompanied by a decrease in fascicle length over time. While speculative, this observation might suggest an increase in sarcomeres in parallel. However, future studies are required to confirm this hypothesis.

The relationship between muscle shear modulus — derived from SW velocity — and muscle force during active muscle contraction has been comprehensively studied (Lima et al., 2017a; Yoshitake et al., 2014). These studies documented a linear relationship between muscle shear modulus and muscle force during submaximal contraction up to 60 % of MVC, with muscle shear modulus measurements showing more accurate estimation of contraction intensity compared to surface electromyography. However, at rest, MG shear modulus was not related to measures of muscle strength or MVC (Lima et al., 2017b), concomitant with the findings of this study.

To our knowledge this is the first study to show an association between tissue SW velocity and fascicle length of the MG muscle. The data indicate that longer MG fascicles are associated with lower SW velocity, reflecting more compliant muscle at rest. Consistent with our observation, there is evidence that longer fascicles in a given muscle are associated with lower passive tension at the single fiber and whole muscle levels at long lengths (Hinks et al., 2022). Furthermore, Andrade et al., (2020) assessed muscle properties using SWE and structural changes in the MG muscle following a 12-week stretching program. They observed a decrease in the MG muscle SW velocity accompanied by an increase in fascicle length. It is plausible to assume that an increase in fascicle length may partly account for decreased muscle stiffness as a long term adaptation following a 12-week stretching program, during which the muscle is tensioned at long lengths (Andrade et al., 2020; Weppler and Magnusson, 2010). Conversely, shorter fascicles may result in increased

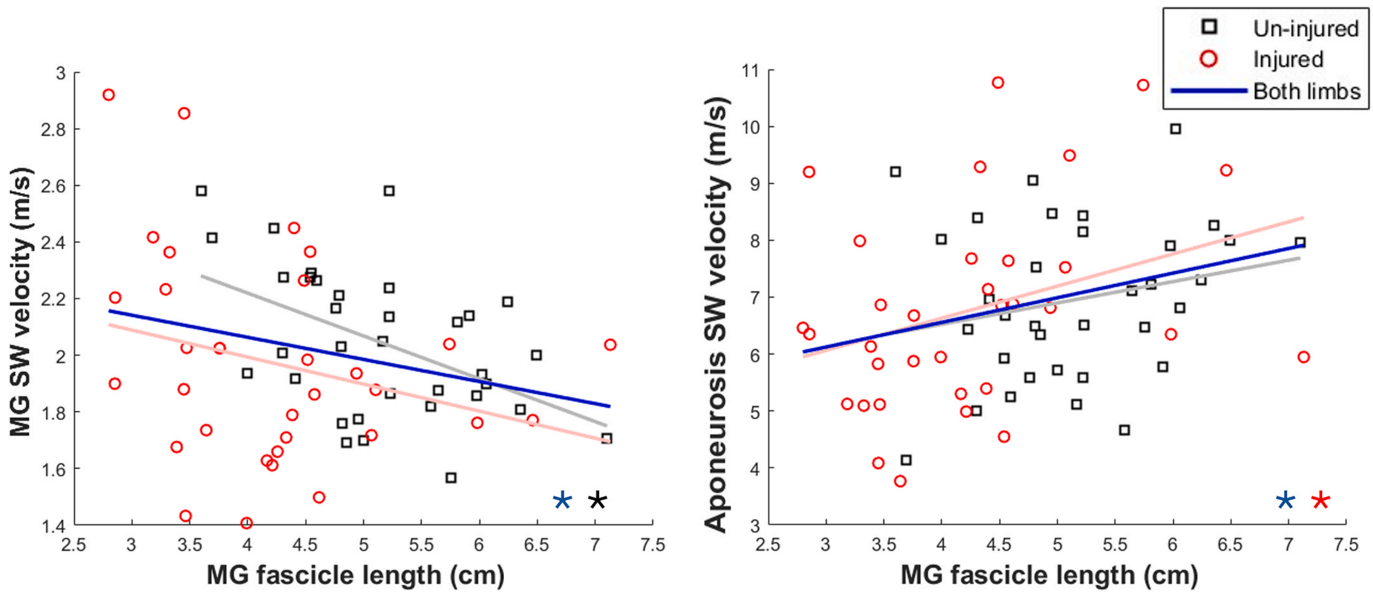

Fig. 4. Scatterplots and regression lines of the correlations between SW velocity of the MG (left) or aponeurosis (right) and MG fascicle length at 6 and 12 months. * Significant correlation $p < 0.05$, * colour coded as follows: black for un-injured limb, red for injured limb, and blue for both limbs combined. (For interpretation of the references to colour in this figure legend, the reader is referred to the web version of this article.)

muscle stiffness after an injury such as ATR, where tendon elongation shifts the tension to shorter MG lengths.

Fascicle length has implications for the force–length relationship (Tabary et al., 1972; Woittiez et al., 1983), and overall mechanical output of the muscle (Cox et al., 2000; Drazan et al., 2019). Theoretically, muscles with longer fascicles can achieve faster excursions over greater ranges and perhaps higher forces (Drazan et al., 2019; Lieber and Fridén, 2000). Indeed, higher SW velocity of the aponeurosis was associated with longer fascicles and higher maximum plantar flexion torque. Considering the role of tendon stiffness in muscle force and rate of torque development (Arampatzis et al., 2007; Monte and Zignoli, 2021; Quinlan et al., 2018), it is reasonable to assume that muscles with longer fascicles and higher force outputs have stiffer aponeuroses, potentially providing structural support for the compliant muscle. However, it is unclear how tissue properties measured at rest reveal information about muscle and tendon properties measured during dynamic contractions or active lengthening. Therefore, the findings of this study warrant careful interpretation.

This study is not without limitations. Due to the nature of ATR, we were not able to have equal representation between sexes, however this does not influence the integrity of the analysis as comparisons were done within participants. The SWE technique is based on the assumption that the measured tissues are linearly elastic, homogenous and isotropic (Bercoff et al., 2004), however these conditions might not be fully met. Therefore, we chose to report SW velocity for both the MG muscle and aponeurosis. Lastly, it should be noted that the AT resting length was measured from the most proximal point of the calcaneus to the MG MTJ. While this measurement may not capture the full anatomical length of the tendon, it is sufficient to detect elongation of the tendon following ATR.

5. Conclusion

After ATR, SW velocity of the MG muscle and aponeurosis were lower at 2 months but recovered to the levels of the un-injured side by 6 months in non-surgically treated patients. The associations observed in this study suggest that remodelling of the MG muscle to shorter fascicle lengths may help restore tension in the injured muscle. However, these changes have consequences, as shorter fascicle length is associated with lower SW velocity at the aponeurosis and lower force production capacity.

CRediT authorship contribution statement

Ra'ad M. Khair: Conceptualization, Data curation, Formal analysis, Investigation, Validation, Visualization, Writing – original draft, Writing – review & editing. **Maria Sukanen:** Writing – review & editing, Data curation, Conceptualization. **Neil J. Cronin:** Writing – review & editing, Supervision. **Taija Finni:** Writing – review & editing, Resources, Project administration, Methodology, Funding acquisition, Conceptualization.

Funding

This work was funded by Academy of Finland research projects UNderstanding REStoration of Achilles Tendon function after rupture (UNRESAT, grant #323168/Taija Finni), and Development of novel methods for creation of a new subject-specific view of Achilles tendon structure and loading in health and disease (ACHILLES, grant #355678/ Taija Finni).

Declaration of competing interest

The authors declare that they have no known competing financial interests or personal relationships that could have appeared to influence the work reported in this paper.

Appendix A. Supplementary data

Supplementary data to this article can be found online at https://doi.org/10.1016/j.jbiomech.2025.112915.

Data availability

The data that support the findings of this study are available upon reasonable request from the authors.

References

Agres, A.N., Duda, G.N., Gehlen, T.J., Arampatzis, A., Taylor, W.R., Manegold, S., 2015. Increased unilateral tendon stiffness and its effect on gait 2–6 years after Achilles tendon rupture. Scand. J. Med. Sci. Sports 25, 860–867. https://doi.org/10.1111/sms.12456.

Akagi, R., Takahashi, H., 2013. Acute effect of static stretching on hardness of the gastrocnemius muscle. Med. Sci. Sports Exerc. 45, 1348. https://doi.org/10.1249/MSS.0b013e3182850e17.

Andrade, R.J., Freitas, S.R., Hug, F., Le Sant, G., Lacourpaille, L., Gross, R., Quillard, J.-B., McNair, P.J., Nordez, A., 2020. Chronic effects of muscle and nerve-directed stretching on tissue mechanics. J. Appl. Physiol. 129, 1011–1023. https://doi.org/10.1152/japplphysiol.00239.2019.

Arampatzis, A., Karamanidis, K., Morey-Klapsing, G., De Monte, G., Stafilidis, S., 2007. Mechanical properties of the triceps surae tendon and aponeurosis in relation to intensity of sport activity. J. Biomech. 40, 1946–1952. https://doi.org/10.1016/j.jbiomech.2006.09.005.

Aubry, S., Risson, J.-R., Barbier-Brion, B., Tatu, L., Vidal, C., Kastler, B., 2011. Élastographie transitoire du tendon calcanéen : résultats préliminaires et perspectives. J. Radiol. 92, 421–427. https://doi.org/10.1016/j.jradio.2011.02.024.

Barfod, K.W., Riecke, A.F., Boesen, A., Hansen, P., Maier, J.F., Døssing, S., Troelsen, A., 2015. Validation of a novel ultrasound measurement of Achilles tendon length. Knee Surg. Sports Traumatol. Arthrosc. 23, 3398–3406.

Baxter, J.R., Hullfish, T.J., Chao, W., 2018. Functional deficits may be explained by plantarflexor remodeling following Achilles tendon rupture repair: preliminary findings. J. Biomech. 79, 238–242. https://doi.org/10.1016/j.jbiomech.2018.08.016.

Bercoff, J., Tanter, M., Fink, M., 2004. Supersonic shear imaging: a new technique for soft tissue elasticity mapping. IEEE Trans. Ultrason. Ferroelectr. Freq. Control 51, 396–409. https://doi.org/10.1109/TUFFC.2004.1295425.

Bernabei, M., Lee, S.S.M., Perreault, E.J., Sandercock, T.G., 2020. Shear wave velocity is sensitive to changes in muscle stiffness that occur independently from changes in force. J. Appl. Physiol. Bethesda Md 1985 (128), 8–16. https://doi.org/10.1152/japplphysiol.00112.2019.

Blazevich, A.J., 2019. Adaptations in the passive mechanical properties of skeletal muscle to altered patterns of use. J. Appl. Physiol. 126, 1483–1491. https://doi.org/10.1152/japplphysiol.00700.2018.

Bohm, S., Mersmann, F., Santuz, A., Schroll, A., Arampatzis, A., 2021. Muscle-specific economy of force generation and efficiency of work production during human running. eLife 10, e67182. https://doi.org/10.7554/eLife.67182.

Bojsen-Møller, J., Magnusson, S.P., Rasmussen, L.R., Kjaer, M., Aagaard, P., 2005. Muscle performance during maximal isometric and dynamic contractions is influenced by the stiffness of the tendinous structures. J. Appl. Physiol. 99, 986–994. https://doi.org/10.1152/japplphysiol.01305.2004.

Bolsterlee, B., Gandevia, S.C., Herbert, R.D., 2016. Ultrasound imaging of the human medial gastrocnemius muscle: how to orient the transducer so that muscle fascicles lie in the image plane. J. Biomech. 49, 1002–1008. https://doi.org/10.1016/j.jbiomech.2016.02.014.

Chen, X.-M., Cui, L.-G., He, P., Shen, W.-W., Qian, Y.-J., Wang, J.-R., 2013. Shear wave elastographic characterization of normal and torn achilles tendons. J. Ultrasound Med. 32, 449–455. https://doi.org/10.7863/jum.2013.32.3.449.

Chino, K., Takahashi, H., 2016. Measurement of gastrocnemius muscle elasticity by shear wave elastography: association with passive ankle joint stiffness and sex differences. Eur. J. Appl. Physiol. 116, 823–830. https://doi.org/10.1007/s00421-016-3339-5.

Coombes, B.K., Tucker, K., Vicenzino, B., Vuvan, V., Mellor, R., Heales, L., Nordez, A., Hug, F., 2018. Achilles and patellar tendinopathy display opposite changes in elastic properties: a shear wave elastography study. Scand. J. Med. Sci. Sports 28, 1201–1208. https://doi.org/10.1111/sms.12986.

Cox, V.M., Williams, P.E., Wright, H., James, R.S., Gillott, K.L., Young, I.S., Goldspink, D. F., 2000. Growth induced by incremental static stretch in adult rabbit latissimus dorsi muscle. Exp. Physiol. 85, 193–202. https://doi.org/10.1111/j.1469-445X.2000.01950.x.

de Boer, M.D., Seynnes, O.R., di Prampero, P.E., Pišot, R., Mekjavić, I.B., Biolo, G., Narici, M.V., 2008. Effect of 5 weeks horizontal bed rest on human muscle thickness and architecture of weight bearing and non-weight bearing muscles. Eur. J. Appl. Physiol. 104, 401–407. https://doi.org/10.1007/s00421-008-0703-0.

DeWall, R.J., Slane, L.C., Lee, K.S., Thelen, D.G., 2014. Spatial variations in Achilles tendon shear wave speed. J. Biomech. 47, 2685–2692. https://doi.org/10.1016/j.jbiomech.2014.05.008.

Drazan, J.F., Hullfish, T.J., Baxter, J.R., 2019. Muscle structure governs joint function: linking natural variation in medial gastrocnemius structure with isokinetic plantar flexor function. Biol. Open 8, bio048520. https://doi.org/10.1242/bio.048520.

Eby, S.F., Song, P., Chen, S., Chen, Q., Greenleaf, J.F., An, K.-N., 2013. Validation of shear wave elastography in skeletal muscle. J. Biomech. 46, 2381–2387. https://doi.org/10.1016/j.jbiomech.2013.07.033.

Epstein, M., Wong, M., Herzog, W., 2006. Should tendon and aponeurosis be considered in series? J. Biomech. 39, 2020–2025.

Ettema, G.J.C., Huijing, P.A., 1994. Skeletal muscle stiffness in static and dynamic contractions. J. Biomech. 27, 1361–1368. https://doi.org/10.1016/0021-9290(94)90045-0.

Finni, T., Cronin, N.J., Mayfield, D., Lichtwark, G.A., Cresswell, A.G., 2017. Effects of muscle activation on shear between human soleus and gastrocnemius muscles. Scand. J. Med. Sci. Sports 27, 26–34.

Finni, T., Komi, P.V., 2002. Two Methods for Estimating Tendinous Tissue Elongation during Human Movement. Doi: 10.1123/jab.18.2.180.

Finni, T., Peter, A., Khair, R., Cronin, N.J., 2022. Tendon length estimates are influenced by tracking location. Eur. J. Appl. Physiol. https://doi.org/10.1007/s00421-022-04958-8.

Hill, A.V., 1953. The mechanics of active muscle. Proc. R. Soc. Lond. Ser. B-Biol. Sci. 141, 104–117.

Hinks, A., Franchi, M.V., Power, G.A., 2022. The influence of longitudinal muscle fascicle growth on mechanical function. J. Appl. Physiol. 133, 87–103. https://doi.org/10.1152/japplphysiol.00114.2022.

Hoeffner, R., Svensson, R.B., Dietrich-Zagonel, F., Schefte, D., Kjær, M., Eliasson, P., Magnusson, S.P., 2023. Muscle fascicle and sarcomere adaptation in response to Achilles tendon elongation in an animal model. J. Appl. Physiol. 135, 326–333. https://doi.org/10.1152/japplphysiol.00040.2023.

Huijing, P.A., 2003. Muscular force transmission necessitates a multilevel integrative approach to the analysis of function of skeletal muscle. Exerc. Sport Sci. Rev. 31, 167–175. https://doi.org/10.1097/00003677-200310000-00003.

Hullfish, T.J., O'Connor, K.M., Baxter, J.R., 2019. Medial gastrocnemius muscle remodeling correlates with reduced plantarflexor kinetics 14 weeks following Achilles tendon rupture. J. Appl. Physiol. Bethesda Md 1985 (127), 1005–1011. https://doi.org/10.1152/japplphysiol.00255.2019.

Khair, R.M., Stenroth, L., Cronin, N.J., Reito, A., Paloneva, J., Finni, T., 2022. Muscle-tendon morphomechanical properties of non-surgically treated Achilles tendon 1-year post-rupture. Clin. Biomech. 92, 105568. https://doi.org/10.1016/j.clinbiomech.2021.105568.

Khair, R.M., Sukanen, M., Finni, T., 2024. Achilles tendon stiffness: influence of measurement methodology. Ultrasound Med. Biol. https://doi.org/10.1016/j.ultrasmedbio.2024.06.005.

Kubo, K., Kanehisa, H., Fukunaga, T., 2001. Is passive stiffness in human muscles related to the elasticity of tendon structures? Eur. J. Appl. Physiol. 85, 226–232. https://doi.org/10.1007/s004210100463.

Lichtwark, G.A., Wilson, A.M., 2008. Optimal muscle fascicle length and tendon stiffness for maximising gastrocnemius efficiency during human walking and running. J. Theor. Biol. 252, 662–673.

Lieber, R.L., Fridén, J., 2000. Functional and clinical significance of skeletal muscle architecture. Muscle Nerve 23, 1647–1666. https://doi.org/10.1002/1097-4598(200011)23:11<1647::AID-MUS1>3.0.CO;2-M.

Lieber, R.L., Leonard, M.E., Brown, C.G., Trestik, C.L., 1991. Frog semitendinosis tendon load-strain and stress-strain properties during passive loading. Am. J. Physiol.-Cell Physiol. 261, C86–C92. https://doi.org/10.1152/ajpcell.1991.261.1.C86.

Lima, K.M.M. e, Júnior, J.F.S.C., Pereira, W.C. de A., Oliveira, L.F. de, 2017. Assessment of the mechanical properties of the muscle-tendon unit by supersonic shear wave imaging elastography: a review. Ultrasonography 37, 3–15. Doi: 10.14366/usg.17017.

Lima, K., Martins, N., Pereira, W., Oliveira, L., 2017b. Triceps surae elasticity modulus measured by shear wave elastography is not correlated to the plantar flexion torque. Muscles Ligaments Tendons J. 7, 347–352. https://doi.org/10.11138/mltj/2017.7.2.347.

Luke, S.G., 2017. Evaluating significance in linear mixed-effects models in R. Behav. Res. Methods 49, 1494–1502. https://doi.org/10.3758/s13428-016-0809-y.

McNair, P., Nordez, A., Olds, M., Young, S.W., Cornu, C., 2013. Biomechanical properties of the plantar flexor muscle–tendon complex 6 months post-rupture of the achilles tendon. J. Orthop. Res. 31, 1469–1474. https://doi.org/10.1002/jor.22381.

Monte, A., Maganaris, C., Baltzopoulos, V., Zamparo, P., 2020. The influence of Achilles tendon mechanical behaviour on "apparent" efficiency during running at different speeds. Eur. J. Appl. Physiol. 120, 2495–2505. https://doi.org/10.1007/s00421-020-04472-9.

Monte, A., Zignoli, A., 2021. Muscle and tendon stiffness and belly gearing positively correlate with rate of torque development during explosive fixed end contractions. J. Biomech. 114, 110110. https://doi.org/10.1016/j.jbiomech.2020.110110.

Quinlan, J.I., Maganaris, C.N., Franchi, M.V., Smith, K., Atherton, P.J., Szewczyk, N.J., Greenhaff, P.L., Phillips, B.E., Blackwell, J.I., Boereboom, C., Williams, J.P., Lund, J., Narici, M.V., 2018. Muscle and tendon contributions to reduced rate of torque development in healthy older males. J. Gerontol. A Biol. Sci. Med. Sci. 73, 539–545. https://doi.org/10.1093/gerona/glx149.

Roberts, T.J., 2016. Contribution of elastic tissues to the mechanics and energetics of muscle function during movement. J. Exp. Biol. 219, 266–275. https://doi.org/10.1242/jeb.124446.

Ross, S.A., Waters-Banker, C., Sawatsky, A., Leonard, T.R., Herzog, W., 2024. A methodological approach for collecting simultaneous measures of muscle, aponeurosis, and tendon behaviour during dynamic contractions. Biol. Open 13, bio060383. https://doi.org/10.1242/bio.060383.

Shin, D.D., Hodgson, J.A., Edgerton, V.R., Sinha, S., 2009. In vivo intramuscular fascicle-aponeuroses dynamics of the human medial gastrocnemius during plantarflexion and dorsiflexion of the foot. J. Appl. Physiol. 107, 1276–1284. https://doi.org/10.1152/japplphysiol.91598.2008.

Stäudle, B., Seynnes, O., Laps, G., Göll, F., Brüggemann, G.-P., Albracht, K., 2020. Recovery from achilles tendon repair: a combination of postsurgery outcomes and insufficient remodeling of muscle and tendon. Med. Sci. Sports Exerc. Publish Ahead of Print. https://doi.org/10.1249/MSS.0000000000002592.

Sukanen, M., Khair, R.M., Reito, A., Ponkilainen, V., Paloneva, J., Cronin, N., Hautala, A. J., Finni, T., 2024. Early predictors of recovery from nonoperatively treated achilles tendon rupture: 1 year follow-up study. Scand. J. Med. Sci. Sports 34, e14700. https://doi.org/10.1111/sms.14700.

Surgeons, A.A., 2009. The Diagnosis and Treatment of Acute Achilles Tendon Rupture: Guideline and Evidence Report. Rosemt. IL Am. Acad. Orthop. Surg.

Tabary, J.C., Tabary, C., Tardieu, C., Tardieu, G., Goldspink, G., 1972. Physiological and structural changes in the cat's soleus muscle due to immobilization at different lengths by plaster casts. J. Physiol. 224, 231–244. https://doi.org/10.1113/jphysiol.1972.sp009891.

Ueno, H., Suga, T., Takao, K., Tanaka, T., Misaki, J., Miyake, Y., Nagano, A., Isaka, T., 2017. Potential relationship between passive plantar flexor stiffness and running

performance. Int. J. Sports Med. 39, 204–209. https://doi.org/10.1055/s-0043-121271.
Weppler, C.H., Magnusson, S.P., 2010. Increasing muscle extensibility: a matter of increasing length or modifying sensation? Phys. Ther. 90, 438–449.
Woittiez, R.D., Huijing, P.A., Rozendal, R.H., 1983. Influence of muscle architecture on the length-force diagram of mammalian muscle. Pflüg. Arch. 399, 275–279. https://doi.org/10.1007/BF00652752.
Yoshida, K., Itoigawa, Y., Morikawa, D., Maruyama, Y., Ishijima, M., 2023. Chronologic changes in the elastic modulus of a healing achilles tendon rupture measured using shear wave elastography. Foot Ankle Int. 44, 243–250. https://doi.org/10.1177/10711007221151083.
Yoshitake, Y., Takai, Y., Kanehisa, H., Shinohara, M., 2014. Muscle shear modulus measured with ultrasound shear-wave elastography across a wide range of contraction intensity. Muscle Nerve 50, 103–113. https://doi.org/10.1002/mus.24104.